NeuroImage 290 (2024) 120574

Contents lists available at ScienceDirect

NeuroImage

journal homepage: www.elsevier.com/locate/ynimg

Opposite changes in morphometric similarity of medial reward and lateral non-reward orbitofrontal cortex circuits in obesity

Debo Dong [a,b,1], Ximei Chen [a,1], Wei Li [a], Xiao Gao [a], Yulin Wang [a,d], Feng Zhou [a], Simon B. Eickhoff [b,c], Hong Chen [a,e,*]

[a] Key Laboratory of Cognition and Personality, Ministry of Education, Faculty of Psychology, Southwest University, Chongqing 400715, China
[b] Institute of Neuroscience and Medicine, Brain & Behaviour (INM-7), Research Centre Jülich, Jülich, Germany
[c] Institute for Systems Neuroscience, Medical Faculty, Heinrich-Heine University Düsseldorf, Düsseldorf, Germany
[d] Sleep and NeuroImaging Center, Faculty of Psychology, Southwest University, Chongqing 400715, China
[e] Research Center of Psychology and Social Development, Faculty of Psychology, Southwest University, Chongqing 400715, China

ARTICLE INFO

Keywords:
Obesity
Body mass index
Morphometric similarity networks
Orbitofrontal cortex
Multimodal MRI

ABSTRACT

Obesity has a profound impact on metabolic health thereby adversely affecting brain structure and function. However, the majority of previous studies used a single structural index to investigate the link between brain structure and body mass index (BMI), which hinders our understanding of structural covariance between regions in obesity. This study aimed to examine the relationship between macroscale cortical organization and BMI using novel morphometric similarity networks (MSNs). The individual MSNs were first constructed from individual eight multimodal cortical morphometric features between brain regions. Then the relationship between BMI and MSNs within the discovery sample of 434 participants was assessed. The key findings were further validated in an independent sample of 192 participants. We observed that the lateral non-reward orbitofrontal cortex (lOFC) exhibited decoupling (i.e., reduction in integration) in obesity, which was mainly manifested by its decoupling with the cognitive systems (i.e., DMN and FPN) while the medial reward orbitofrontal cortex (mOFC) showed de-differentiation (i.e., decrease in distinctiveness) in obesity, which was mainly represented by its de-differentiation with the cognitive and attention systems (i.e., DMN and VAN). Additionally, the lOFC showed de-differentiation with the visual system in obesity, while the mOFC showed decoupling with the visual system and hyper-coupling with the sensory-motor system in obesity. As an important first step in revealing the role of underlying structural covariance in body mass variability, the present study presents a novel mechanism that underlies the reward-control interaction imbalance in obesity, thus can inform future weight-management approaches.

1. Introduction

According to the World Health Organization (2024), the global population of adults who were overweight totaled more than 2.5 billion. Of this group, over 890 million were categorized as obese. A growing obesity epidemic poses a grave threat to public health. Obesity has been found to be closely linked to chronic conditions such as type 2 diabetes, hyperlipidemia, high blood pressure, cardiovascular disease, and cancer (Kivimäki et al., 2022). Indeed, obesity results in 2.8 million premature deaths worldwide annually. Yet, treatments rarely result in lasting weight loss and virtually all obesity prevention programs have not reduced future obesity onset (Plotnikoff et al., 2015; Stice et al., 2006). Understanding the neurobiology associated with obesity is crucial as it can unveil the underlying brain mechanisms that drive overeating and weight gain, offering precise targets for intervention. By identifying these neural correlates, we can develop more effective treatments and preventive strategies that are tailored to modify specific neural pathways, leading to more successful long-term outcomes in managing obesity. Despite significant efforts, neural correlates of obesity are not yet sufficiently defined, which hinders our understanding of

* Corresponding author at: Key Laboratory of Cognition and Personality, Ministry of Education, Faculty of Psychology, Southwest University, Chongqing 400715, China.
E-mail address: chenhg@swu.edu.cn (H. Chen).
[1] These two authors contributed equally to this work.

https://doi.org/10.1016/j.neuroimage.2024.120574
Received 9 December 2023; Received in revised form 5 March 2024; Accepted 8 March 2024
Available online 10 March 2024

neurobiology associated with obesity (Stice and Burger, 2019; Stice and Yokum, 2016) and further limits the development of new effective intervention.

Empirically, neurostructural alterations have been demonstrated in individuals with obesity and individual variations of body mass index (BMI) in non-clinical conditions, including abnormalities in gray matter volume (Hamer and Batty, 2019; Herrmann et al., 2019; Opel et al., 2017), white matter microstructure (Daoust et al., 2021; Okudzhava et al., 2022), cortical thickness (Laurent et al., 2020; Ronan et al., 2020), and deformations in subcortical shape (Kim et al., 2020). These findings suggest a particular important role of neurobiological alterations involved in executive functioning and reward processing (phenotypes) in overweight and obesity (for reviews, see Li et al. 2023, Lowe et al. 2020, 2019, Stice and Burger 2019). This is further supported by findings from resting-state fMRI studies, which suggest that problematic eating behaviors in obesity are associated with disrupted communication between reward, inhibitory, and homeostatic systems (Parsons et al., 2022; Syan et al., 2021).

Based on the various strands of evidence from the obesity literature, it is evident that the orbitofrontal cortex (OFC) plays a pivotal role in obesity-related brain alterations (Rolls, 2023; Seabrook and Borgland, 2020; Stice and Burger, 2019; Syan et al., 2021). Several meta-analyses have consistently reported that individuals with obesity exhibit a reduction in the volume of the orbitofrontal cortex (OFC), marking it as a notable structural brain abnormality in this population (Chen et al., 2020; García-García et al., 2019; Zapparoli et al., 2022). The OFC is crucial in representing the reward value and subjective pleasantness of food-related sensory experiences such as taste, smell, sight, and touch in primates, including humans (Rolls, 2023). Meta-analytical evidence indicates that obese individuals demonstrate increased activity in the orbitofrontal cortex (OFC) and ventral striatum, brain regions involved in taste and reward processing, in response to food-related stimuli (Devoto et al., 2018). Furthermore, recent research indicates that even in a resting state, without direct food-related cues, there is a link between an individual's food preferences (which are likely to influence body mass index) and the functional connectivity between the OFC and the ventromedial prefrontal cortex (Rolls et al., 2023b). This finding suggests that variations in the reward systems of the orbitofrontal cortex may contribute to personal differences in how food is perceived as pleasant and in the propensity for obesity (Rolls, 2023; Seabrook and Borgland, 2020).

However, previous structural studies often focused on single structural index, which does not allow for detection of alterations in structural covariance between brain regions in obesity. Structural covariance characterizes how morphologic properties of brain regions are related to one another across individuals, which represent a reliable way to construct the macroscale cortical structural organization. It has been posited that the topology of structural covariance provides an important source of constraint for the organization of human cognition (Han et al., 2023b; Valk et al., 2020). However, traditional structural covariance networks often produce group-level networks that reflect population-level covariance in neuroanatomy. This approach limits the capability to identify and quantify system-level abnormalities at the individual level. Additionally, accurately estimating long-distance connections remains a challenge for diffusion-weighted imaging (DTI)--based tractography. This limitation stems from the inherent difficulty in tracking the complex pathways of white matter fibers over extended distances in the brain (Zhang et al., 2021b).

In a significant advancement towards understanding the large-scale organization of the cortex, Seidlitz et al. (2018) introduced an innovative approach for constructing an individual-based morphometric similarity matrix. This method leverages a variety of morphometric features across different modalities to characterize the structural covariance between brain regions. Unlike previous techniques that relied on the inter-regional correlation of a single MRI feature across subjects, this methodology estimates "connections" – essentially, structural similarities – by using newly introduced feature vectors. These vectors are created by calculating the Pearson correlation coefficient across concatenated morphometric features, offering a more nuanced view of brain structure than methods focusing on one or two anatomical features. Brain regions in which the feature vectors correlate when measured across a large set of individuals are said to have "high connectivity", though in fact this represents high covariation of structure (Li et al., 2017). Such combined analysis of multiple indices has been found to be more effective than that of a single morphometric index at each region (Glasser and Van Essen, 2011; Michel et al., 2024; Sabuncu et al., 2016; Seidlitz et al., 2018; Vandekar et al., 2016; Whitaker et al., 2016). Meanwhile, this method of constructing individual-based morphometric similarity networks (MSNs) has successfully improved the accuracy of discriminant analysis (Yu et al., 2018).

To the best of our knowledge, the MSNs have been used to characterize morphometric similarity changing patterns in major depressive disorder (Li et al., 2021), schizophrenia (Morgan et al., 2019), and Alzheimer's disease (Zhang et al., 2021b), as well as to predict brain age (Galdi et al., 2020) and variance in IQ (Seidlitz et al., 2018), and individual differences in inhibitory control (He et al., 2020). Although MSN is a reliable and robust method for capturing the greater spatial congruence with cortical cytoarchitecture than networks derived from diffusion imaging or those based on a singular structural metric, such as cortical thickness (Seidlitz et al., 2018), this technique has yet to be usedto uncover morphometric covariance associated with obesity in adulthood. Previous studies have confirmed the aberrant functionality of the brain networks/circuits underlying obesity (for reviews, see Li et al. 2023, Schlögl et al. 2016). Given that structural connectivity and functional connectivity seem to show positive correlations, in those regions of the brain that are highly structurally interconnected tend to exhibit strong patterns of functional connectivity (for a review, see Uddin 2013), we speculate that neuroanatomical features measured by MSNs will be linked with body mass variability.

The aim of this work, therefore, was to examine the potential association between individualized MSNs and obesity from a multi-morphometric perspective. We first modeled inter-regional correlations of multiple macro- and micro-structural multi-contrast MRI variables (here, neuroanatomical features were measured by individual-based MSNs constructed from cortical characteristic indexes between the brain regions) in a single individual within a discovery dataset (HCP cohort, $n = 434$ unrelated participants). We then examined whether BMI (i.e., a simple and common index of weight-for-height that reflects overweight and obesity) is related to individual brain structure similarity patterns. Additionally, we tested the replicability of the BMI-related MSN variations in an independent validation dataset (AOMIC cohort, $n = 192$) by performing a category strategy (96 obese vs. 96 normal weight). Given the converging lines of evidence highlighting a crucial role of OFC circuit in obesity, as mentioned above, we hypothesized that variations in BMI among individuals would be associated with changes in the morphometric similarity of the orbitofrontal cortex (OFC). This hypothesis is grounded in the understanding that the OFC's structural and functional characteristics are closely linked to the neural mechanisms underlying food reward processing and preference, which in turn, may influence obesity risk. As mentioned earlier, previous structural studies on obesity have typically concentrated on single structural indices, which limited our ability to discern changes in structural covariance between brain regions. In contrast, our current study employs the innovative approach of using MSNs to detect alterations in the structural covariance among brain regions associated with obesity. This approach would offer new insights into the neuroanatomical basis of obesity, enriching our understanding beyond what was possible with traditional methods. Such advancements may contribute to the development of targeted psychological and clinical interventions to promote weight loss.

2. Methods

2.1. Participants and multi-neuroimaging data acquisition

2.1.1. Discovery sample: human connectome project (HCP) dataset

Participants included in this study were selected from the 1200 Subjects Release (S1200) dataset of the HCP (Van Essen et al., 2013). For HCP dataset, the core group of participants is sourced from healthy young (aged 22–35) individuals born in Missouri from twin-inclusive families, according to information from the Missouri Department of Health and Senior Services Bureau of Vital Records. Extra recruitment measures were implemented to ensure that the participant demographic closely represents the ethnic and racial diversity of the U.S. population, as depicted in the 2000 decennial census. The HCP adopts a wide-ranging definition of 'healthy' to establish a participant base that is representative of the general population. This strategy is intended to capture a broad spectrum of variation among healthy individuals in terms of behavioral, ethnic, and socioeconomic factors. Further details can be obtained from the HCP1200 data release manual (https://www.humanconnectome.org/documentation/S1200/). All procedures involving human subjects were approved by the Ethics Committee of the local HCP institute. This study was carried out in accordance with the Declaration of Helsinki. Written informed consents were obtained from all subjects. We excluded data from 78 participants based on the exclusion criteria indicated as follows: (1) participants with missing T1-weighted structural MRI (sMRI) and diffusion MRI (dMRI) images (n = 48); (2) participants with missing values on demographic variables such as BMI, age, sex, education, and race (n = 3) or family information (family identification number, n = 3); (3) participants with a history of hyper/hypothyroidism (n = 4) or history of other endocrine problems (n = 16), due to the confounding effects these conditions have on obesity, which could confound the results (Reinehr, 2010); and (4) women who had recently given birth (n = 4, Gunderson (2009)).

To this end, we obtained a total of 1035 participants from 434 families. Considering the BMI is highly heritable (ranging from 0.47 to 0.90, Elks et al., 2012), we randomly selected one participant from each family to eliminate the heritability influence. Finally, 434 participants for which multimodal images and BMI were used for the current analyses were included (females, 234 [53.90 %]; age, 28.85 ± 3.60; BMI, 26.46 ± 5.24, see Table 1 for details).

Image data of all subjects from the HCP were scanned on a customized 3T scanner at Washington University (WashU). The MRI data consisted of T1-weighted structural MRI (sMRI) and diffusion MRI (dMRI). Images were acquired on a customized 3T Skyra scanner (Siemens, Erlangen, Germany) with a standard 32-channel head coil (Van Essen et al., 2013). A T1-weighted sMRI was acquired using a magnetization-prepared rapid gradient echo (MPRAGE) sequence (repetition time (TR) = 2400 ms, echo time (TE) = 2.14 ms, inversion time = 1000 ms, flip angle (FA) = 8°, field of view (FOV) = 224 × 224 mm^2, 0.7 mm^3 isotropic resolution).

Diffusion MRI (dMRI) data were acquired using a Spin-echo EPI sequence. A full dMRI session includes six runs, representing three different gradient tables, with each table acquired once with right-to-left and left to-right phase encoding polarities, respectively. Each gradient table includes approximately 90 diffusion weighting directions plus 6 b = 0 acquisitions interspersed throughout each run. Diffusion weighting consisted of 3 shells of b = 1000, 2000, and 3000 s/mm^2 interspersed with an approximately equal number of acquisitions on each shell within each run (TR = 5520 ms, TE = 89.5 ms, FA = 78°, FOV = 210 × 180 mm^2, matrix size = 168 × 144 mm^2, 1.25 mm^3 isotropic resolution).

All procedures involving human subjects were approved by the Ethics Committee of the Southwest University.

2.1.2. External validation sample: Amsterdam Open MRI Collection (AOMIC)

To test whether the significant association results from the HCP sample can be directly validated in obese sample using an independent sample, we downloaded Amsterdam Open MRI Collection (AOMIC) to use as an external validation dataset. For the AOMIC dataset, subjects were recruited through a recruitment firm (Motivaction International B. V.) with the aim of creating a sample reflective of the general population of the Netherlands in terms of education level (as categorized by the Dutch government17), while restricting the age group to 19 to 26 years. This narrow age bracket was chosen to reduce the influence of aging on brain-related variables. All procedures involving human subjects were approved by the Ethics Committee of the local AOMIC institute. This study was carried out in accordance with the Declaration of Helsinki. Written informed consent forms were obtained from all subjects. From AOMIC, we focused on the ID1000 dataset, which is a representative young sample of the Dutch population, similar to the HCP sample (Snoek et al., 2021). We excluded 24 participants with missing diffusion MRI (dMRI) images and demographic variables such as BMI, age, sex, and education. Among the remaining 904 participants, we further excluded participants with underweight (BMI<18.5) and obtained 574 normal-weight (18.5≤BMI<24.5) and 96 obese participants (BMI≥30). Propensity score matching based on age, sex, and educational level was applied to minimize the demographic differences between normal weight and obese groups in these aspects to reduce the bias and confounding factors from demographics (Stuart and Green, 2008). Optimal

Table 1
Demographic information of discovery and validation sample.

Discovery sample: HCP		Validation sample: AOMIC		
		Obese group (Ob)	Normal weight group (NW)	Statistics (Ob vs NW)
N	434	96	96	
Body Mass Index (BMI), mean (SD), Kg/M^2	26.46 (5.24)	33.83 (3.98)	21.81(1.59)	$t = 27.46$, $p < 0.0001$
Age, mean (SD), years	28.85 (3.60)	23.24 (1.59)	23.23(1.61)	$t = 0.05$, $p = 0.964$
Female (Sex), N (%)	234 (53.92)	59(61.36)	59(61.36)	$X^2=0$, $p = 1$
Education, mean (SD), years	14.94 (1.80)	Level 1 = 18 Level 2 = 52 Level 3 = 26	Level 1 = 19 Level 2 = 49 Level 3 = 28	$X^2=0.19$, $p = 0.91$
Handedness, mean (SD) [a]	65.47 (45.27)	–	–	
Total household income	see notes for detials	–	–	
Employment status (%)		–	–	
not working	61 (14.05)			
part-time employment	77 (17.74)			
full-time employment	296 (68.21)			
Ethnicity (%)		–	–	
Hispanic/Latino	50(11.52)	–	–	
Not Hispanic/Latino	384 (88.48)	–	–	
Race N (%)		–	–	
White	319 (73.50)	–	–	
Other[b]	115 (26.50)	–	–	

Notes: Total household income for HCP dataset: <$10,000 (29, 6.68 %),10K-19,999 (35, 8.06 %), 20K-29,999 (49, 11.29 %),30K-39,999 (52, 11.98 %), 40K-49,999 (44, 10.14 %), 50K-74,999 (103, 23.73 %), 75K-99,999 (55, 12.67 %), >=100,000 (67, 15.44 %). [a]Handedness of participants from -100 to 100 is assessed using the Edinburgh Handedness questionnaire. [b]Other than white, including 67 Black or African American, 35 Asian/Nat. Hawaiian/Othr Pacific Is and 13 more than one race. Level 1=low; Level 2= medium; Level 3=high. Level of education was defined by the Central Bureau van de Statistiek, CBS.

matching with probit propensity scores was conducted in the MatchIt package Version 4.5.2 (Ho et al., 2011) in R (Version 4.2.1) and resulted in a final sample of 96 obese participants and 96 well-matched normal weight participants with all P values larger than 0.9. See Table 1 for details.

Image data from AOMIC were acquired on the same Philips 3 T scanner-"Intera" version (Philips, Best, the Netherlands). Three high-resolution T1-weighted images were acquired using a MPRAGE sequence (TR = 8.2 ms, TE = 3.8 ms, FA = 8, FOV = 256 × 256 mm^2, 1 mm^3 isotropic resolution). Given the relatively low signal-to-noise ratio of diffusion data, three diffusion weighted imaging measurements were acquired (TR = 6312 ms, TE = 73.36 ms, FA = 90°, FOV = 224 × 112 mm^2, 60 transversal slices of 2 mm, 32 directions, b0 = 1000s/mm^2).

All procedures involving analyzing data of human subjects from the HCP and AOMIC were approved by the Ethics Committee of the Southwest University.

2.2. Data preprocessing

For the HCP dataset, structural data preprocessing included three pipelines. The first structural pipeline, *PreFreeSurfer*, aimed to produce an undistorted "native" structural volume space for each subject, align the T1-weighted and T2-weighted images, perform a B_1 (bias field) correction, and register the subject's native structural volume space to the Montreal Neurological Institute (MNI) space. The second pipeline, *FreeSurfer 5.3.0*, segmented the volume into predefined structures, reconstructed white and pial cortical surfaces, and performed FreeSurfer's standard folding-based surface registration to their surface atlas. The final structural pipeline, *PostFreeSurfer*, produced all of the NIFTI volume and GIFTI surface files, applying the surface registration. The diffusion preprocessing pipeline included the following steps: normalized the b_0 image intensity across runs; removed EPI distortions, eddy-current-induced distortions, and subject motion; corrected for gradient-nonlinearities; registered the diffusion data with the structural; brought it into 1.25 mm structural space; and masked the data with the final brain mask. The quality control of all the released processed data was conducted by HCP group. For a detailed description of data preprocessing, refer to Glasser et al. (2013). After preprocessing, diffusion tensor models were estimated using weighted linear least squares fitting. From the estimated tensor image, a fractional anisotropy (FA) image was computed.

For the AOMIC dataset, the T1-weight images were corrected for intensity non-uniformity, skull-stripped, and reconstructed brain surface using recon-all (FreeSurfer v6.0.1). The brain mask estimated previously was refined with a custom variation of the method. Spatial normalization to the ICBM 152 Nonlinear Asymmetrical template was achieved through nonlinear registration. Brain tissue segmented into cerebrospinal fluid, white-matter, and gray-matter. Diffusion images were preprocessed using a custom pipeline that combines tools from MRtrix3 and FSL v6.0. Multiple dMRI scans, diffusion gradient table and b-value information were concatenated prior to preprocessing. The diffusion data was denoised, Gibbs ringing artifacts were removed, and eddy current and motion correction were performed. Within eddy, a quadratic first-level and linear second-level model were performed and outlier replacement was performed with default parameters. Then, bias correction was performed, a brain mask was extracted, and possible issues with the diffusion gradient table were corrected. After preprocessing, a diffusion tensor model was fit on the preprocessed data using weighted linear least squares via MRtrix3. From the estimated tensor image, a fractional anisotropy (FA) image was computed. The quality control of all the released processed data was conducted by AOMIC group. For a detailed description of the data preprocessing, please refer to Snoek et al. (2021).

2.3. Construction of MSN

The same MSN construction procedures were used for discovery and replication datasets. To ensure comparability with prior research on morphometric similarity networks (Li et al., 2021; Morgan et al., 2019; Seidlitz et al., 2018), we adopted the Desikan-Killiany atlas in the current study. Utilizing the same atlas facilitates a direct comparison between our MSN pattern and the previously published MSN pattern by Morgan et al. (2019). Specifically, the cortical surfaces were divided into 308 spatially contiguous regions derived from the 68 cortical regions in the Desikan-Killiany atlas. This parcellation produced regions of approximately equal size (~500 mm^2) using a backtracking algorithm using a backtracking algorithm, as previously described (Romero-Garcia et al., 2012). This approach minimizes the influence of the variability in parcel sizes (Li et al., 2021; Morgan et al., 2019; Seidlitz et al., 2018). This parcellated Desikan-Killiany atlas was transformed to each participant's surface to obtain an individual surface parcellation, which was then interpolated and expanded to the participant's DWI volumes. For each region, eight features (available for both datasets) from the processed T1-weighted and DWI images were extracted, including cortical thickness (CT), surface area (SA), gray matter volume (GM), mean curvature (MC), intrinsic (Gaussian) curvature (GC), curved index (CI), folding index (FI), and fractional anisotropy (FA). Previous studies have demonstrated that these eight cortical metrics are closely associated with each other, providing complementary information about specific regions of the cerebral cortex (King and Wood, 2020; Morgan et al., 2019; Seidlitz et al., 2018). Specifically, cortical thickness provides the information of the thickness of the outer layer of the cerebral cortex. Surface area refers to the surface of the cerebral cortex, the outer layer of the brain, providing information about cortical folding patterns. Gray matter volume provides important information about the overall structural characteristics of the brain. Mean curvature provides information about the curvature or bending of a cortical surface at each point, thus indicating local folding. Intrinsic (Gaussian) curvature provides information about the local geometry and curvature of a surface. The curvedness index provides information about the local curvature at each point on a surface. This information helps characterize how much a surface deviates from being flat or planar at specific locations. Folding index refers to a measure that quantifies the amount of cortical folding or gyrification of the brain. Higher levels of folding or gyrification typically suggest a greater surface area, allowing for more neurons and synaptic connections. Fractional anisotropy refers to scalar that quantifies the extent of directional constraint on the diffusion of water molecules; it is sensitive to the colinearity of the axonal fibers and provides a representation of white matter integrity.

For each participant, eight features (available for both datasets) in each region were *z*-normalized. Pearson's correlation analysis was then performed on the morphometric features between each paired region, which was compiled to form a 308 × 308 MSN for each participant (Fig. 1).

To test the robustness of MSN construction, we performed a reduction in the number of morphometric features available for analysis. Here, the leave-one-feature-out approach was used: we calculated the correlation between the MSN constructed with all the eight features (CT, SA, GM, MC, IC, CI, FI, and FA) and the MSN constructed with one feature left out (for example, leave the CT out) for each subject. Then, we averaged the correlations across participants. Additionally, we examined the stability of the current 8-feature MSNs by comparing them to the commonly used 5-feature MSNs (Yang et al., 2021). The 5-feature MSNs refers to a reduced set of 5 morphometric features that can be derived from T1-weighted MRI scans: CT, SA, GM, MC, and IC.

2.4. Statistical analyses

At the regional level, we first calculated the regional MSN values (i.e., regional degree) as the sum of weighted correlation coefficients

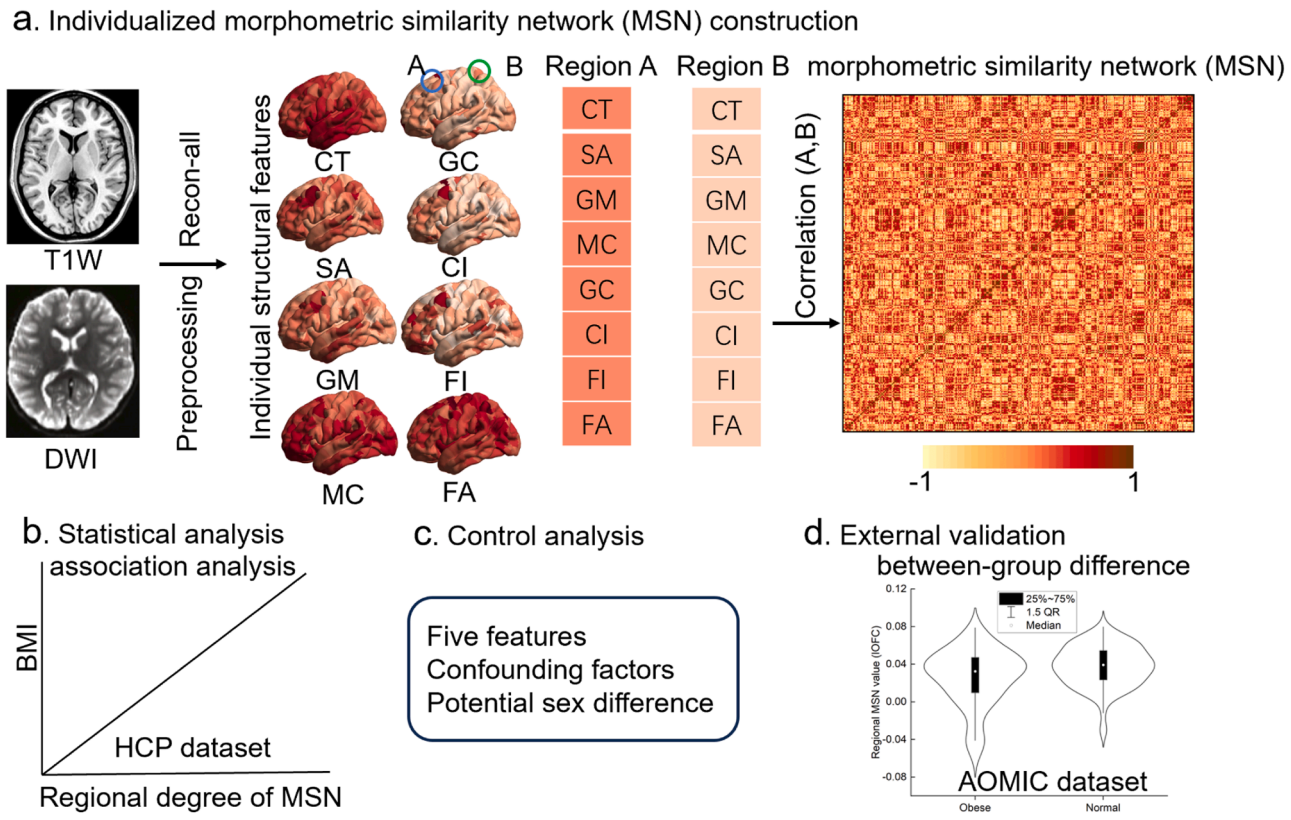

Fig. 1. Analysis flowchart. (a) Individualized morphometric similarity network (MSN) construction. (b) Linear regression analysis in HCP dataset. (c) Control analysis. (d) d. External validation: between-group difference was conducted in AOMIC dataset.

between a given region and all other regions. Then, the association between BMI and regional MSN values was investigated using linear regression analyses adjusting for age, sex, years of education, handedness, race (categorized as white or other than white), and total intracranial volume (TIV) in the regression models. To obtain robust results, we used a permutation analysis of linear models (PALM; Winkler et al. 2014) to determine the significance for all correlational analyses. To correct for the impact of multiple comparisons, we applied the false discovery rate (FDR) correction method. A p-value of less than 0.05, after FDR correction, was considered significant. At the edge level, we further conducted the seed-based structural 'connectivity' analyses (i.e., one column in the 308 × 308 MSN matrix) to detect the detailed structural covariance between the regions identified by the regional analysis above and other rest regions to account for individual variations of BMI.

2.5. Control analysis

We validated the main findings by considering several control analyses. Given the known sex differences in obesity and at the brain level, sex was included as a covariate in our analysis. However, to further elucidate the relationship, we conducted additional analyses to test if the association between BMI and our main findings in regional MSN differs significantly between sexes. Fisher's Z-Transformation test was used to test whether the correlations between BMI and regional MSN observed in main analysis in males and females statistically different. Relatedly, we also carried out a control analysis to determine whether our primary findings concerning regional MSN are significantly associated with the number of days since the last menstrual period in female participants with regular cycles ($N = 198$). Additionally, we accounted for other potential socioeconomic status (such as household income and employment status) and ethnicity in our association analysis model. Finally, we validated our main results by considering only 5 morphometric features derived from T1 data.

2.6. External validation: AOMIC dataset

A between-group difference analysis was conducted on regions showing significant regional morphometric similarity in the discovery dataset. These regions were then used as seeds to analyze the abnormal structural covariance in the obese group compared to the normal BMI group. Age, sex, education, and TIV were adjusted in the regression models.

3. Results

3.1. Robustness and stability of MSN construction

Regarding the stability of nodal similarity, averaged correlations for all the eight are notably high. Specifically, the average r of leaving CI out is 0.94; the average r of leaving CT out is 0.91; the average r of leaving FA out is 0.92; the average r of leaving FI out is 0.98; the average r of leaving GC out is 0.91; the average r of leaving GM out is 0.99; the average r of leaving MC out is 0.93; the average r of leaving SA out is 0.96. In addition, we found a high correlation ($r = 0.84$) in the sample mean regional values (mean map) between the current 8-feature MSNs and a 7-feature MSNs recently reported by Morgan et al. (2019).

In terms of the stability of edge weights, averaged correlations for all the eight are notably high as well. Specifically, the average r of leaving CI out is 0.99; the average r of leaving CT out is 0.92; the average r of leaving FA out is 0.92; the average r of leaving FI out is 0.98; the average r of leaving GC out is 0.98; the average r of leaving GM out is 0.99; the average r of leaving MC out is 0.96; the average r of leaving SA out is 0.96. These results demonstrated the high robustness of the morphometric similarity method in relation to the exclusion of any individual feature.

We further observed strong similarity between the 5-feature MSNs and the 8-feature MSNs. Specifically, the sample mean edge weights and nodal similarities were highly correlated ($r = 0.823$, $p < 0.001$ for edge weights; $r = 0.943$, $p < 0.001$ for nodal similarities). However, the standard deviations (*SD*) for both edge weights and nodal similarity were higher in the 5-feature MSNs (0.332 and 0.022, respectively) compared to the 8-feature MSNs (0.290 and 0.018, respectively), This suggests the estimation of MSN is more precise when based on a larger number of parameters. Therefore, we opted for the 8-feature MSNs for the subsequent analyses.

3.2. Association between BMI and MSNs

3.2.1. At the regional level: nodal degree

The cortical map depicted in Fig. 2a illustrates the anatomical distribution of areas with positive and negative similarity in the discovery dataset, which is based on average value from participants with normal weight). This map highlights areas of high positive morphometric similarity predominantly in frontal and temporal cortex, while areas with high negative morphometric similarity are observed in the occipital, somatosensory, and motor cortex. The patterns align with findings from previous independent studies (Morgan et al., 2019; Seidlitz et al., 2018), underscoring its replicability. Furthermore, the observed distribution pattern is consistent with existing knowledge, indicating that the primary cortex exhibits a higher level of histological differentiation compared to the association cortex.

We identified a significant positive correlation between BMI and regional morphometric similarity in the bilateral medial orbitofrontal cortex (left mOFC1 (centroid (MNI): X=-6, $Y = 17$, Z=-17;right mOFC2 (centroid (MNI): $X = 7$, $Y = 19$, Z=-18)), as well as negative correlations between BMI and regional morphometric similarity in the lateral orbitofrontal cortex (lOFC, centroid (MNI): X=−29, $Y = 25$, Z=-13) and bilateral postcentral gyrus (all $p_{FDR} < 0.05$, centroid (MNI): X=-16, Y=-36, $Z = 71$; $X = 14$, Y=-35, $Z = 72$) as shown in Fig. 2b and c). These findings suggested an increased morphometric similarity in the mOFC and decreased morphometric similarity in the lOFC and postcentral gyrus among individuals with higher BMI. To illustrate these relationships, significant regions were plotted on the average regional MSN map derived from individuals with normal weight (Fig. 2d). The observed positive regional *r*-values alongside negative mean MSN in mPFC indicated a de-differentiation of this area in individuals with higher BMI. Conversly, negative regional *r*-value with positive mean MSN in lOFC suggested a decoupling of this area in individuals with higher BMI. Similarly, negative regional *r*-value accompanied by negative mean MSN in postcentral gyrus indicated a hyper-differentiation of this area in individuals with higher BMI.

3.2.2. At the network level: mOFC- and lOFC-based structural 'connectivity'

To delve deeper into the specific structural covariance patterns associated with the observed morphometric changes in individuals with higher BMI, particularly the general de-differentiation observed in the mOFC, decoupling in the lOFC, and hyper-differentiation in the postcentral gyrus, we conducted the seed-based structural 'connectivity' analyses. This involved examining one column in the 308 × 308 MSN matrix. The aim was to detect the detailed structural covariance between these regions and the rest of the brain, thereby shedding light on how individual variations in BMI are associated with changes in the brain's

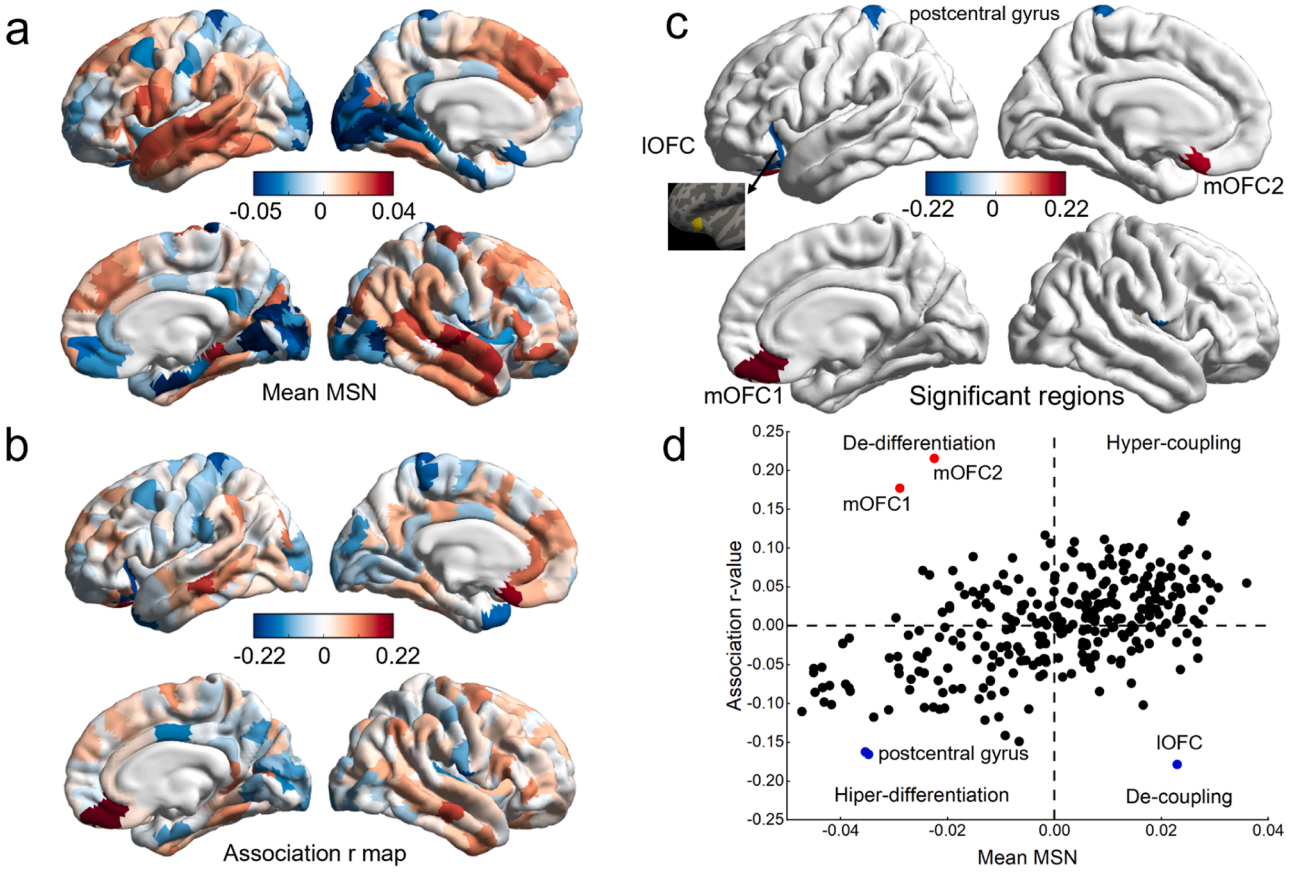

Fig. 2. Associations between body mass index and regional morphometric similarity. (a) Averaged regional morphometric similarity across all normal weight participants. (b) r statistics for the associations between body mass index and regional morphometric similarity. (c) Significant associations between body mass index and regional morphometric similarity. FDR corrected $p < 0.05$) (d) Scatterplot of mean regional morphometric similarity of all normal weight participants (x axis) vs. association r statistic (y axis).

structural network.

In the context of network neuroscience, de-differentiation refers to the process where previously distinct and specialized neural networks or brain regions become less unique, showing more overlap in their functions. Decoupling refers to the reduction of the functional connectivity or interaction between different brain regions or networks.

With the lOFC as the seed, the mean pattern across subjects showed that lOFC mainly coupled with cognitive systems, such as the frontal, temporal, and parietal cortex, while differentiated from limbic, sensorimotor, and visual systems (Fig. 3a). To contextualize the further finding of association between BMI and seed-based structural covariance into network level, the positive and negative association edges were further summarized by the number of edges within large-scale functional networks (Fig. 3b) according to Yeo's seven networks (Yeo et al., 2011). To test whether the number of edges in each within network is not randomly distributed, we conducted 5000 spatial permutation tests to obtain a null distribution of the number of edges within each network while accounting for the spatial autocorrelation of brain regions (Burt et al., 2020). Specifically, we employed a "spin"-based approach to address potential confounding effects associated with spatial autocorrelation. The spin test, a spatial permutation method (Váša et al., 2018), operates through angular permutations of spherical projections on the cortical surface. It is important to note that the spin test maintains the spatial covariance structure of the data, making it a considerably more conservative approach than randomly shuffling locations. In contrast to the latter, which disrupts the spatial covariance structure and yields an unrealistically unconservative null distribution, the spin test ensures the preservation of the inherent spatial relationships within the data. Then, the p_{spin} values were determined by comparison to the null models. We found individuals' BMI was (1) negatively related to connections between the lOFC and cognitive systems (DMN, frontoparietal network [FPN]), indicating a decoupling pattern; and (2) positively related to connections between lOFC and visual systems, indicating a de-differentiation pattern (Fig. 3b).

In contrast, with the mOFC as a seed, the mean pattern across subjects showed that the mOFC mainly coupled with limbic, sensorimotor, and visual systems, while differentiated from other cognitive systems, such as the frontal, temporal, and parietal cortex (Figs. 4a and 5a). Spatial correlation analysis further showed that there was a significant negative correlation between the lOFC and the mOFC seed-based covariance profile (Fig. 6), suggesting opposite patterns. The statistical significance of a spatial correlation was also determined by 5000 spatial permutation tests. In contrast to the result of lOFC seed-based structural covariance. We found BMI was (1) negatively related to connections between the mOFC and the visual system, suggesting a decoupling pattern; (2) positively related to connections between the mOFC and sensorimotor system, suggesting a hypercoupling pattern; and (3) positively related to connections between mOFC and both the default mode network (DMN) and the ventral attention network (VAN), suggesting a de-differentiation pattern (Figs. 4b and 5b).

When taking postcentral gyrus as seed, we did not observe any significant results with FDR correction.

3.3. Control analysis

Our main findings were further validated by several control analyses. Firstly, we examined the influence of sex the correlation between BMI and regional MSN by comparing these correlations in males and females. The results indicated no statistically significant differences (all p values > 0.1, Table S1), suggesting that sex does not significantly impact our findings regarding regional MSN. Additionally, among female participants with regular menstrual cycles, we investigated the potential effect of the menstrual cycle phase by correlating the number of days since the last period with regional MSN in our study. No significant correlations were found (all p values > 0.05, Table S2), indicating that menstrual cycle phase does not significantly affect the regional MSN results in our study. The inclusion of variables related to socioeconomic status and ethnicity did not significantly alter the primary findings, as illustrated in Fig. S1, suggesting that socioeconomic status and ethnicity do not confound our main results. Finally, we employed five morphometric features derived from T1-weighted MRI data to construct the MSNs. Analyses based on these morphometric features confirmed the

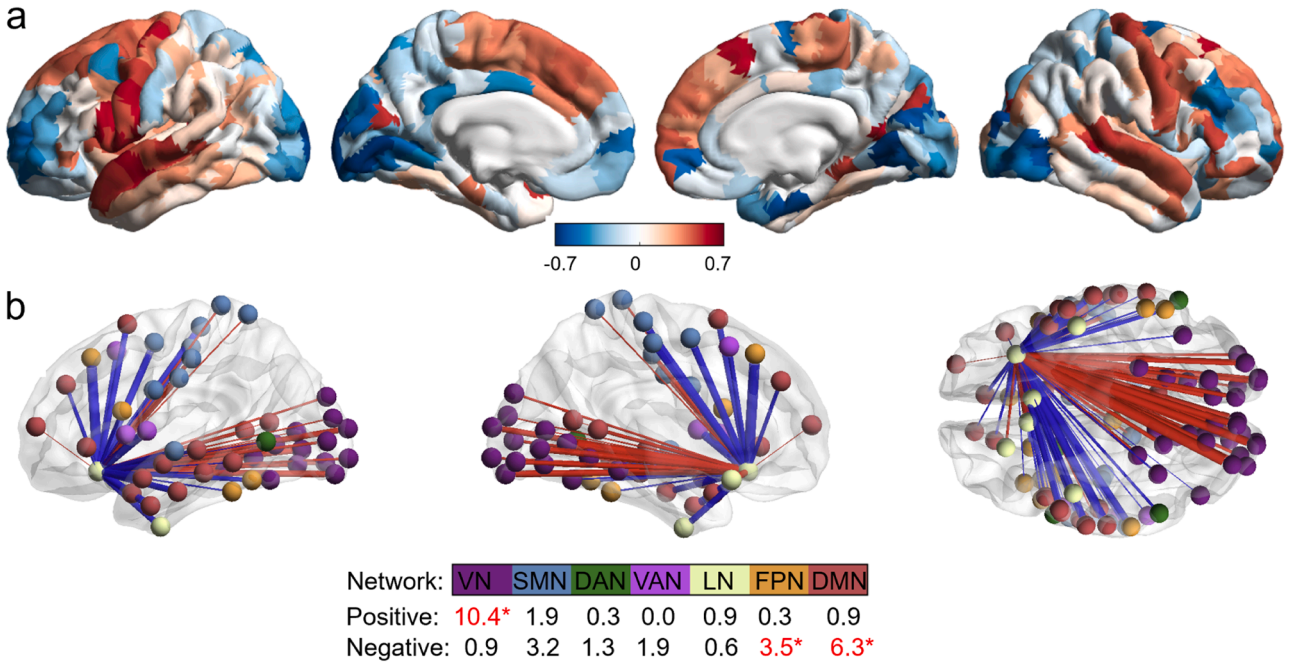

Fig. 3. Associations between body mass index and lOFC seed-based structural covariance. (a) Averaged lOFC seed-based morphometric similarity across all normal weight participants. (b) Significant associations between body mass index and lOFC seed-based morphometric similarity. FDR corrected $p < 0.05$). VN=visual network; SMN=Somatomotor network; DAN=Dorsal attention network; VAN=Ventral attention network; LN=Limbic network; FPN=Frontoparietal network; DMN=Default mode network. *The number of edges in corresponding network are not randomly distributed.

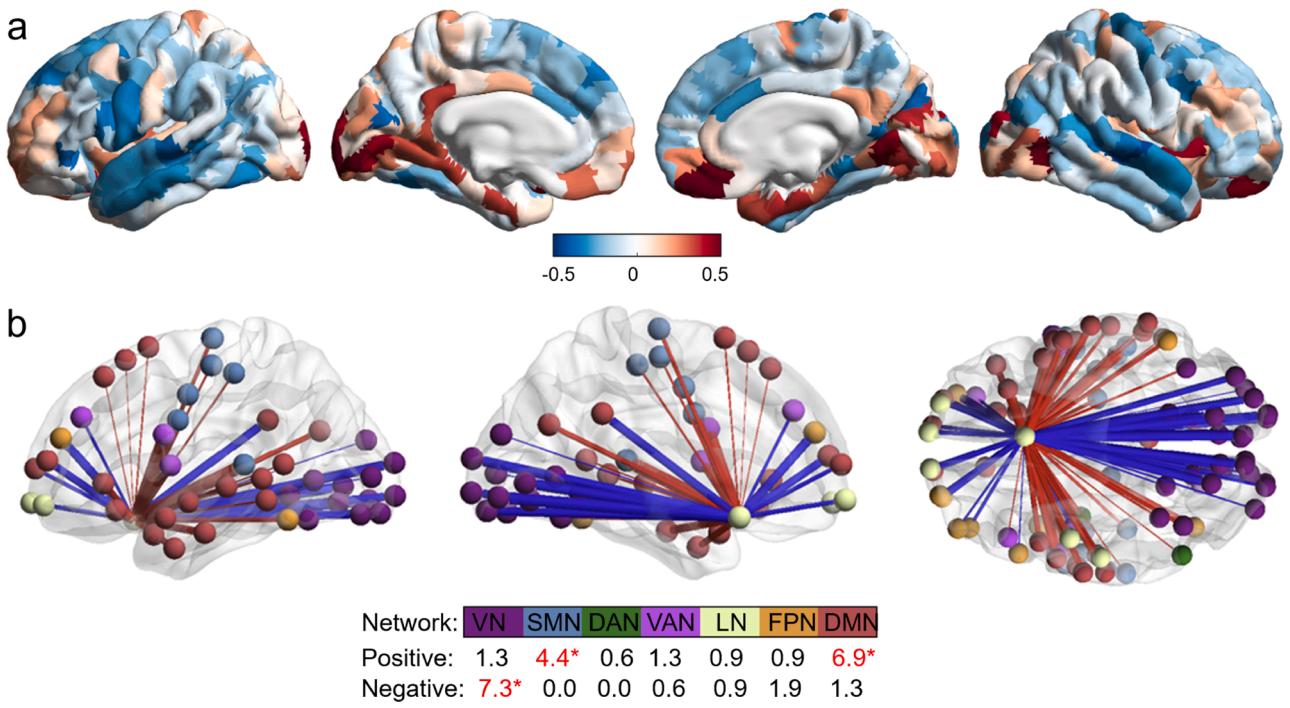

Fig. 4. Associations between body mass index and mOFC seed-based structural covariance. (a) Averaged mOFC1 seed-based morphometric similarity across all normal weight participants. (b) Significant associations between body mass index and mOFC1 seed-based morphometric similarity. FDR corrected $p < 0.05$). VN=visual network; SMN=Somatomotor network; DAN=Dorsal attention network; VAN=Ventral attention network; LN=Limbic network; FPN=Frontoparietal network; DMN=Default mode network. *The number of edges in corresponding network are not randomly distributed.

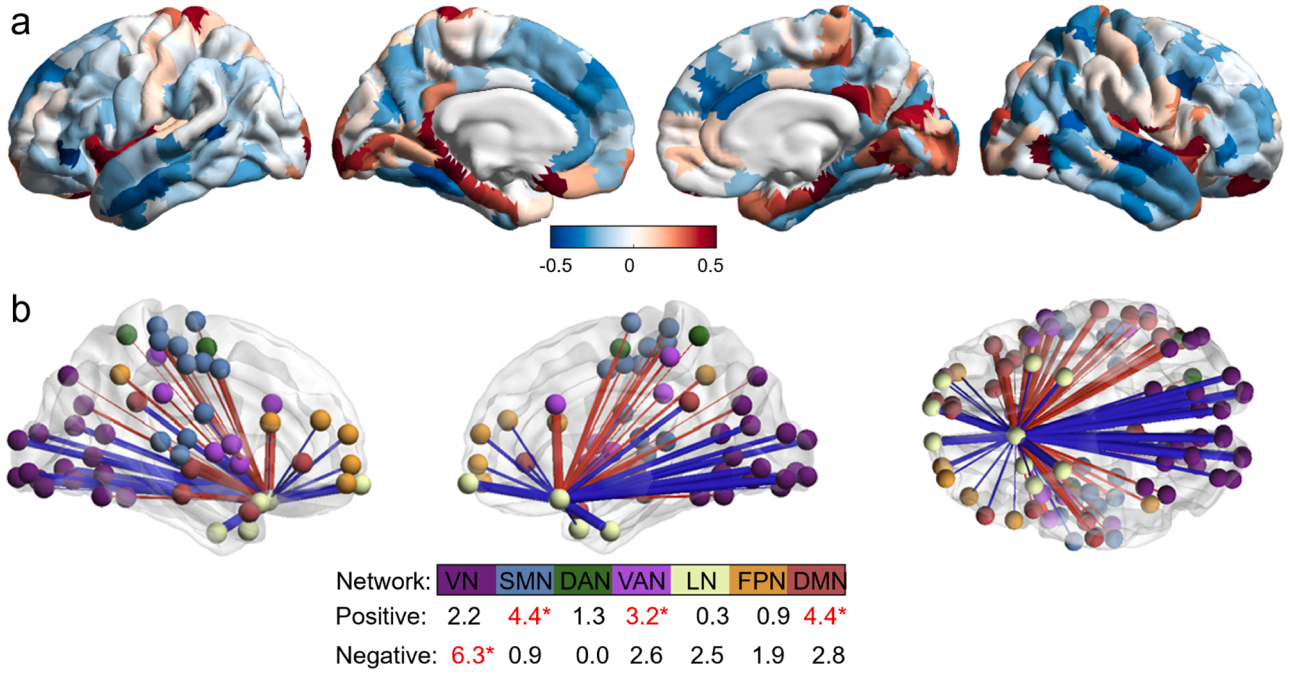

Fig. 5. Associations between body mass index and mOFC2 seed-based structural covariance. (a) Averaged mOFC2 seed-based morphometric similarity across all normal weight participants. (b) Significant associations between body mass index and mOFC2 seed-based morphometric similarity. FDR corrected $p < 0.05$). VN=visual network; SMN=Somatomotor network; DAN=Dorsal attention network; VAN=Ventral attention network; LN=Limbic network; FPN=Frontoparietal network; DMN=Default mode network. *The number of edges in corresponding network are not randomly distributed.

robustness of our primary findings, as indicated by the unaltered results shown in Fig. S2. However, we additionally found, at regional level, BMI was negatively associated with the similarity of the occipital cortex (Fig. S2); at the network level, BMI was negatively associated with similarity between the lOFC and somatomotor network. As indicated in 'Robustness and stability of MSN construction' section, greater precision of MSN estimation can be achieved based on more parameters. Therefore, we regarded MSNs constructed with eight features as the main

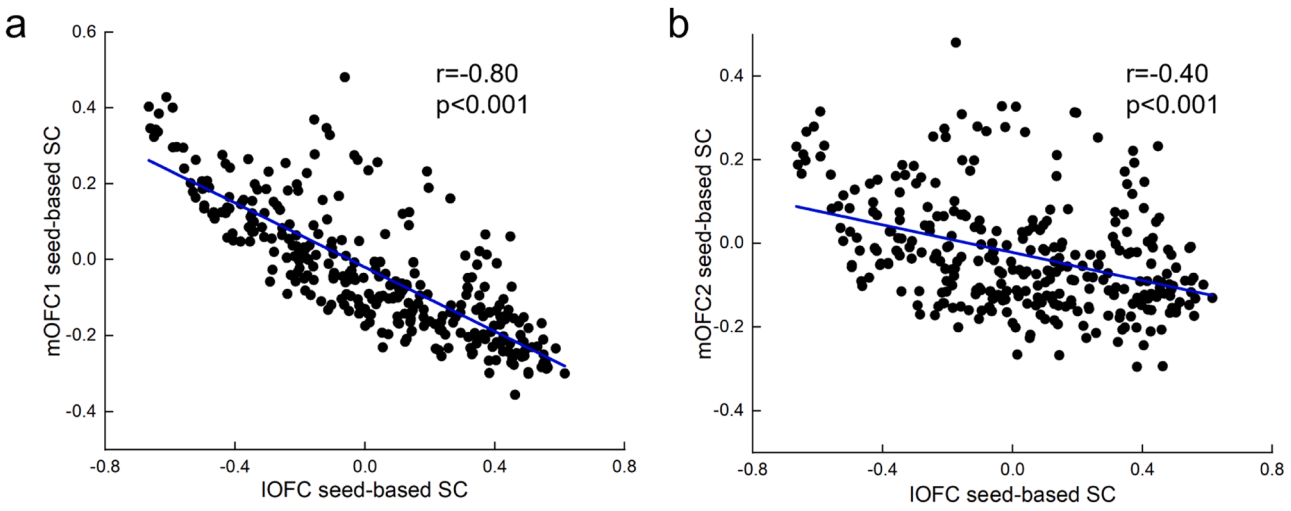

Fig. 6. Spatial correlation between lOFC seed-based SC and mOFC seed-based SC. (a) Negative spatial correlation between lOFC seed-based SC and mOFC1 seed-based SC. (b) Negative spatial correlation between lOFC seed-based SC and mOFC2 seed-based SC.

results.

3.4. Validation analysis on an independent dataset

Similar to findings observed in the discovery HCP dataset, in an independent AOMIC validation dataset, we found that the obese group showed increased regional similarity in mOFC2 and decreased regional similarity in lOFC compared to normal weight group (Fig. 7a and d). Also, the general results of lOFC and mOFC seed-based structural covariance in the AOMIC dataset were similar to those observed in the HCP dataset, as evidenced by significant spatial correlations between them (Fig. 7b,c and e,f). These results thus provided evidence for the robustness of the main findings.

4. Discussion

This study represents an important first step in depicting how structural similarity or covariance between brain regions changes with individual differences of obesity, using MSNs, a robust new structural organization method. We found strong evidence that the ventral medial

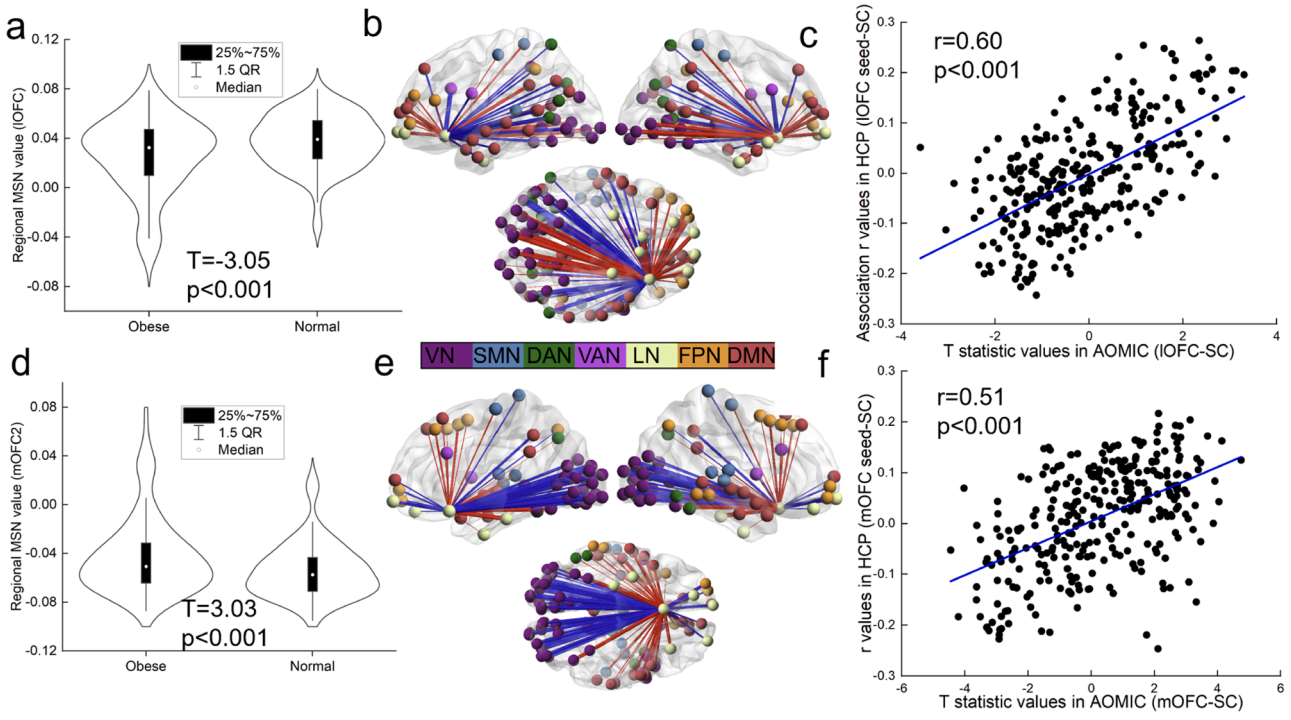

Fig. 7. validation in an independent dataset. (a) Significantly decreased coupling of lOFC in obese group compared with normal weight group. Error bar represents 95 % confidence intervals. (b) Group difference between obese and normal weight group in lOFC seed-based SC. Top 100 edges only for visualization. (c) Significant spatial correlation between r statistics (between BMI and lOFC seed-based SC) in HCP and T statistic value (Obese vs Normal weight) in AOMIC. (d) Significantly decreased de-differentiation of mOFC2 in obese group compared with normal weight group. Error bar represents 95 % confidence intervals. (e) Group difference between obese and normal weight group in mOFC2 seed-based SC. Top 100 edges only for visualization. (f) Significant spatial correlation between r statistics (between BMI and mOFC2 seed-based SC) in HCP and T statistic value (Obese vs Normal weight) in AOMIC. VN=visual network; SMN=Somatomotor network; DAN=Dorsal attention network; VAN=Ventral attention network; LN=Limbic network; FPN=Frontoparietal network; DMN=Default mode network.

reward and lateral non-reward OFC circuits showed opposite changes of morphometric similarity in individual variations of obesity. Specifically, the lOFC showed decoupling in obesity, which was manifested by its decoupling with the cognitive systems including DMN and FPN. Whereas mOFC showed de-differentiation in obesity, this was primarily represented by its de-differentiation with cognitive and attention systems, including DMN and VAN. In addition, mOFC showed decoupling with the visual system, and hypercoupling with the sensorimotor system in obesity, while the lOFC showed de-differentiation with the visual system in obesity. The external validation results provided the robustness of our major findings, suggesting that OFC-related neuroanatomical similarity contributing to body mass variability is sensitive in distinguishing obese and normal individuals. These findings together provided novel neural mechanism to support the reward-control interaction imbalance theory in obesity (Lowe et al., 2020, 2019), with the hope of guiding development of novel and effective treatments for obesity.

The OFC plays a vital role in processing and integrating sensory information, emotion, and reward-related signals to guide goal-directed behavior (Knudsen and Wallis, 2022). It is widely accepted that the OFC can be subdivided into several distinct cytoarchitectonic areas, each with unique connectivity patterns and functional properties. A burgeoning body of research has delved into the nuanced functional distinctions among the subregions of the OFC (Noonan et al., 2010; Wang et al., 2022).Within this intricate landscape, the medial OFC emerges as a key subregion, which is particularly relevant to hot executive functions such as the evaluation of reward and punishment outcomes, as well as in the representation of subjective value (Friedman and Robbins, 2022; Kringelbach and Rolls, 2004; McClure et al., 2007; Salehinejad et al., 2021). The mOFC is also densely interconnected with other brain regions involved in emotional processing, such as the amygdala, and is crucial for integrating emotional and cognitive information to make adaptive decisions (Rolls et al., 2023a). In contrast, the lateral OFC, a part of the lateral prefrontal cortex, is more closely linked to cold executive functions such as flexible decision-making and inhibitory control (Friedman and Robbins, 2022; Kringelbach and Rolls, 2004; McClure et al., 2007; Salehinejad et al., 2021). Lesions or dysfunction in the lOFC have been linked to deficits in impulse control and the ability to adjust behavior based on changing contingencies (Mar et al., 2011). Consistent with the functional distinction between lOFC and mOFC, we found, with lOFC as the seed, the mean pattern across subjects showed that lOFC mainly coupled with cognitive systems, such as frontal, temporal, and parietal cortex, while differentiated from limbic, sensorimotor, and visual systems. Interestingly, the pattern is reversed for mOFC as the seed. Therefore, our seed-based connection analysis provided novel structural evidence to support that the lOFC and mOFC have dissociable connection patterns with the rest of the brain.

Recent structural neuroimaging studies reported that increased BMI was associated with reduced cortical thickness in lOFC, which is associated with diminished executive function (Laurent et al., 2020; Ronan et al., 2020). The present study extended these findings by characterizing the morphometric similarity and found that higher BMI was correlated with lesser morphometric similarity in the lOFC. Prior work has demonstrated that cortical regions that are similar in terms of their morphology are more likely to be axonally connected to each other (Wei et al., 2018), indicating that morphological similarity can serve as an indicator of anatomical connectivity (Seidlitz et al., 2018). A decreased regional MSN of lOFC in individuals with increased BMI implied decreased morphometric similarity or greater morphometric decoupling between lOFC and the rest of the cortex, which can be interpreted as reduced anatomical connectivity to and from the less similar, more differentiated cortical areas (Li et al., 2021). We further observed that BMI was negatively related to the coupling between lOFC and the higher-order cognitive systems (DMN and FPN). It has been suggested that the DMN is a task-negative network that underlies self-referential thinking, memory encoding and retrieval, and social reasoning (Greicius et al., 2003), while the FPN is a major task-positive network, which supports executive functioning such as working memory, impulse control, and goal-oriented cognition (Barkhof et al., 2014). Given that overweight and obesity are considered to be linked to aberrant inhibitory control, cognitive flexibility (Bauer and Houston, 2017; Lips et al., 2014; Yang et al., 2018), and self-directed thinking (Zhang et al., 2021a), our results thus provided novel anatomical evidence supporting the decreased dietary self-control (as indicated by a decoupling pattern between lOFC and FPN), as well as abnormal interaction between food intake control and self-focused and body-focused ruminations (i.e., a decoupling pattern between lOFC and DMN) in adults with a high BMI.

Interestingly, the mOFC showed the opposite changes of morphometric similarity in individual variations of obesity. Specifically, a higher BMI was significantly related to increased regional morphometric similarity in the mOFC, as well as strengthened structural connectivity (i.e., weaker differentiation) between mOFC and cognitive and attention systems (DMN and VAN). The mOFC is responsible for rewarding functions, including reward-based eating drive and reward sensitivity (Li et al., 2022). Furthermore, altered brain structure in the mOFC, such as gray matter volume and cortical thickness, has been associated with binge eating (Smith et al., 2021; Zhang et al., 2021c) and obesity (Marqués-Iturria et al., 2013; Smucny et al., 2012). A positive correlation between BMI and regional morphometric similarity in the mOFC extended previous sMRI findings (Marqués-Iturria et al., 2013; Smucny et al., 2012) by demonstrating decreased morphometric differentiation between mOFC and the rest of the cortex in individual with higher BMI. It has been suggested that the involvement of cognitive and attention systems (DMN and VAN) may represent the crucial neural substrates that can explain the role of internal mental awareness and attentional processes in overweight and obesity (Sadler et al., 2018; Wang et al., 2023). Theoretically, the brain's reward and high-order cognitive regions (for example, OFC and PFC) play an important role in excessive food intake and obesity (for reviews, see Lowe et al. 2020, 2019). Notably, previous research has demonstrated that the neural correlates of inhibition and reward are negatively correlated and proposed that abnormal association between inhibitory and reward circuitry may be a prospective marker of risk for impulsive and addictive behaviors (Weafer et al., 2019). Therefore, enhanced structural covariance between the mOFC and cognitive systems, manifesting as weaker differentiation between them, can be reflective of an aberrant interaction between reward reactivity and inhibitory control in adults with a high level of BMI.

This study expands on the previous work in this area (for reviews, see Chen et al. 2020, Li et al. 2023, Nota et al. 2020, Stice and Burger 2019) by using a recently developed morphometric similarity mapping approach to examine how human cortical structural covariance networks underpin individual differences in BMI. It reveals that the medial reward and lateral non-reward OFC circuits showed opposite changes of regional morphometric similarity in obesity. Notably, the structural covariance of lOFC/mOFC with primary systems also exhibited opposite directions. The lOFC showed de-differentiation with the visual and sensorimotor systems in obesity (a positive relationship of BMI with connections between lOFC and visual and sensorimotor networks). However, the mOFC exhibited decoupling with visual system, and hypercoupling with sensorimotor system in obesity (a negative relationship of BMI with connections within the visual network, and a positive relationship with connections within sensorimotor network). There is evidence that functional connectivity measured when participants were drinking a milkshake could effectively predict waist circumference, indicating the importance of connectivity between sensory processing systems (visual and motor networks) and higher-order systems (subcortical, cingulo-opercular, and default networks) in characterizing body mass variability (Farruggia et al., 2020). Thus, our current results may suggest that information integration between the high-order and primary regions/networks could explain the potential interactions of dysfunctional reward/inhibition functions with visual processing of food cues in obesity (Farruggia et al., 2020; Wang et al.,

2023).

Bariatric surgery is the most effective treatment for clinical obesity (Arterburn et al., 2020). Other interventions and treatments including dietary (Chao et al., 2021), exercise (Carraça et al., 2021), pharmacological (May et al., 2020), and neuromodulation such as transcranial direct current stimulation and neurofeedback (Gouveia et al., 2021) are also used and have achieved promising outcomes (Li et al., 2023). These interventions appeared to normalize hyper- and hypoactivations of brain regions involved in food-intake control, cognitive function, and reward processing, and also promote recovery of brain structural abnormalities (for a review, see Li et al. 2023). However, most of them focused on a single psychological function (i.e., inhibition, reward, or body awareness). In fact, intervention measures targeting a combination of executive functions (e.g., updating, inhibiting, and shifting) have been found to be more effective than those focused on one function (Hofmann et al., 2012). Together with the findings of the present study, future research can further integrate reward-related and food intake control-related factors into specific weight loss interventions.

The left dorsolateral prefrontal cortex (DLPFC) has been widely recognized as a primary target for modulation in previous noninvasive brain stimulation studies in obesity literature (De Klerk et al., 2023; Zeng et al., 2021). Despite this recognition, it is essential to acknowledge that interventions aimed at this specific region remain largely experimental, with the efficacy of these intervention yet to be firmly established (Li et al., 2023; Zeng et al., 2021). The morphometric differences observed in the mOFC, associated with reward, and the lOFC, linked to non-reward, among individuals with obesity suggest a promising alternative for noninvasive brain stimulation interventions. Focusing on noninvasive brain stimulation for both medial and lateral OFC presents a dual-targeted strategy. It aims to modulate neural pathways related to both reward and non-reward processes. This approach aligns with the complex interplay between reward and non-reward circuits in obesity (Lowe et al., 2020, 2019). Simultaneously addressing both reward and non-reward aspects through noninvasive brain stimulation has the potential to induce more lasting changes, promoting successful weight reduction outcomes.

Some limitations of this study should be noted. First, although BMI has been generally considered an index of body fatness, it may be a poorer predictor for cardiovascular risk than waist circumference and waist-to-height ratio (Farruggia et al., 2020; Yan et al., 2007). Future studies could apply waist circumference and waist-to-height ratio, or combine multiple indicators to construct a more comprehensive and accurate indicator to further reveal its neural markers. Second, since this study is cross-sectional, our results cannot establish a causal relationship. Therefore, future longitudinal studies are needed to investigate whether the relevant MSNs discovered in this study can predict changes in BMI. Third, we only considered the linear relationship between BMI and MSN; however, complex brain networks may require nonlinear explanations, which may be enhanced by algorithm optimization in future studies. Finally, despite the homogeneous external phenotypes observed in obese individuals, the causes of obesity are complex and may be driven by various neurobiological factors (Field et al., 2013; Stice and Burger, 2019). Given that MSN recapitulates fundamental properties of cortical organization - including gene expression and cyto- and myeloarchitecture to evolutionary expansion (Yang et al., 2021), the MSN has the potential to be applied as a “brain fingerprint” to distinguish different subtypes of obesity in the future (Han et al., 2023a). As subcortical regions typically exhibit only grey matter volume, MSN is limited in its ability to construct similarity measures between subcortical regions or between cortical and subcortical regions. Since MSNs rely on multiple MRI parameters, the absence of additional morphometric data in subcortical areas hinders the comprehensive assessment needed for constructing meaningful anatomical networks in these regions. With technological advancements, particularly in multi-parametric MRI, future research can further explore the structural similarities of subcortical regions.

5. Conclusions

This study revealed opposite changes in morphometric similarity of the medial reward and lateral non-reward OFC circuits in obesity. As an important first step in revealing the role of underlying structural covariance in body mass variability, the present study presents a novel mechanism that underlies the reward-control interaction imbalance in obesity. It underscores the importance of incorporating aspects associated with both the food reward and the regulation of food intake into specialized weight loss interventions, suggesting a comprehensive approach to tackle obesity. Additionally, the discovery of convergence in the OFC offers novel targets for weight loss interventions through noninvasive brain stimulation, expanding beyond the traditional focus on the left DLPFC. Future longitudinal studies are crucial in order to understand the dynamic nature of these observed changes over time. Specifically, it is important to investigate whether these morphometric alterations in the OFC circuits are a cause or a consequence of obesity. This distinction is critical for developing targeted weight-management interventions.

Data and code availability statement

The discovery data was open access at https://db.humanconnectome.org. The validation data was open access at https://openneuro.org/datasets/ds003097/versions/1.2.1. The code used to transform parcellated Desikan-Killiany atlas to each participant’s native surface is available at https://github.com/RafaelRomeroGarcia/subParcellation. The codes for MSN analysis are openly available at https://github.com/SarahMorgan/Morphometric_Similarity_SZ. The code for spatial permutation testing can be found at https://github.com/frantisekvasa/rotate_parcellation. The brain maps were visualized using ENIGMA toolbox (v2.0.0, Larivière et al., 2021, https://enigma-toolbox.readthedocs.io/en/latest/index.html) and BrainNet Viewer (Xia et al., 2013, https://www.nitrc.org/projects/bnv).

CRediT authorship contribution statement

Debo Dong: Writing – original draft, Investigation, Project administration, Visualization, Funding acquisition, Formal analysis, Data curation, Conceptualization. **Ximei Chen:** Writing – review & editing, Methodology, Investigation, Formal analysis, Data curation. **Wei Li:** Writing – review & editing, Validation, Methodology, Data curation. **Xiao Gao:** Writing – review & editing, Methodology. **Yulin Wang:** Writing – review & editing, Visualization, Methodology. **Feng Zhou:** Writing – review & editing, Methodology. **Simon B. Eickhoff:** Writing – review & editing, Methodology. **Hong Chen:** Writing – review & editing, Supervision, Resources, Conceptualization, Methodology, Funding acquisition.

Declaration of competing interest

The authors declare that they have no conflict of interest.

Acknowledgments

This work was supported by the National Natural Science Foundation of China (Grant No’s. 82202247 and 32271087) and the Major Program of Science and Technology Innovation 2030 by the Ministry of Science and Technology of China (2021ZD0200530), and Natural Science Foundation of Chongqing Municipality (No. 2023NSCQ-MSX4446) and Fundamental Research Funds for the Central Universities (No. SWU2209505).

Supplementary materials

Supplementary material associated with this article can be found, in

the online version, at doi:10.1016/j.neuroimage.2024.120574.

References

Arterburn, D.E., Telem, D.A., Kushner, R.F., Courcoulas, A.P., 2020. Benefits and risks of bariatric surgery in adults: a review. JAMA 324 (9), 879–887. https://doi.org/10.1001/jama.2020.12567.

Barkhof, F., Haller, S., Rombouts, S.A., 2014. Resting-state functional MR imaging: a new window to the brain. Radiology 272, 29–49. https://doi.org/10.1148/radiol.14132388.

Bauer, L.O., Houston, R.J., 2017. The value of instability: an investigation of intrasubject variability in brain activity among obese adolescent girls. Int. J. Obes. 41, 1489–1495. https://doi.org/10.1038/ijo.2017.144.

Burt, J.B., Helmer, M., Shinn, M., Anticevic, A., Murray, J.D., 2020. Generative modeling of brain maps with spatial autocorrelation. Neuroimage 220, 117038. https://doi.org/10.1016/j.neuroimage.2020.117038.

Carraça, E.V., Encantado, J., Battista, F., Beaulieu, K., Blundell, J.E., Busetto, L., van Baak, M., Dicker, D., Ermolao, A., Farpour-Lambert, N., Pramono, A., Woodward, E., Bellicha, A., Oppert, J.M., 2021. Effect of exercise training on psychological outcomes in adults with overweight or obesity: a systematic review and meta-analysis. Obes. Rev. 22, e13261. https://doi.org/10.1111/obr.13261.

Chao, A.M., Quigley, K.M., Wadden, T.A., 2021. Dietary interventions for obesity: clinical and mechanistic findings. J. Clin. Investig. 131 (1), e140065 https://doi.org/10.1172/JCI140065.

Chen, E.Y., Eickhoff, S.B., Giovannetti, T., Smith, D.V., 2020. Obesity is associated with reduced orbitofrontal cortex volume: a coordinate-based meta-analysis. NeuroImage Clin 28, 102420. https://doi.org/10.1016/j.nicl.2020.102420.

Daoust, J., Schaffer, J., Zeighami, Y., Dagher, A., Garcia-Garcia, I., Michaud, A., 2021. White matter integrity differences in obesity: a meta-analysis of diffusion tensor imaging studies. Neurosci. Biobehav. Rev. 129, 133–141. https://doi.org/10.1016/j.neubiorev.2021.07.020.

De Klerk, M., Smeets, P., la Fleur, S., 2023. Inhibitory control as a potential treatment target for obesity. Nutr. Neurosci. 26, 429–444. https://doi.org/10.1080/1028415X.2022.2053406.

Devoto, F., Zapparoli, L., Bonandrini, R., Berlingeri, M., Ferrulli, A., Luzi, L., Banfi, G., Paulesu, E., 2018. Hungry brains: a meta-analytical review of brain activation imaging studies on food perception and appetite in obese individuals. Neurosci. Biobehav. Rev. 94, 271–285. https://doi.org/10.1016/j.neubiorev.2018.07.017.

Elks, C.E., Den Hoed, M., Zhao, J.H., Sharp, S.J., Wareham, N.J., Loos, R.J., Ong, K.K., 2012. Variability in the heritability of body mass index: a systematic review and meta-regression. Front. Endocrinol. 3 (29) https://doi.org/10.3389/fendo.2012.00029.

Farruggia, M.C., van Kooten, M.J., Perszyk, E.E., Burke, M.V., Scheinost, D., Constable, R.T., Small, D.M., 2020. Identification of a brain fingerprint for overweight and obesity. Physiol. Behav. 222, 112940 https://doi.org/10.1016/j.physbeh.2020.112940.

Field, A.E., Camargo, C.A., Ogino, S., 2013. The merits of subtyping obesity: one size does not fit all. JAMA 310, 2147–2148. https://doi.org/10.1001/jama.2013.281501.

Friedman, N.P., Robbins, T.W., 2022. The role of prefrontal cortex in cognitive control and executive function. Neuropsychopharmacology 47, 72–89. https://doi.org/10.1038/s41386-021-01132-0.

Galdi, P., Blesa, M., Stoye, D.Q., Sullivan, G., Lamb, G.J., Quigley, A.J., Thrippleton, M. J., Bastin, M.E., Boardman, J.P., 2020. Neonatal morphometric similarity mapping for predicting brain age and characterizing neuroanatomic variation associated with preterm birth. NeuroImage Clin. 25, 102195 https://doi.org/10.1016/j.nicl.2020.102195.

García-García, I., Michaud, A., Dadar, M., Zeighami, Y., Neseliler, S., Collins, D.L., Evans, A.C., Dagher, A., 2019. Neuroanatomical differences in obesity: meta-analytic findings and their validation in an independent dataset. Int. J. Obes. 43, 943–951. https://doi.org/10.1038/s41366-018-0164-4.

Glasser, M.F., Van Essen, D.C., 2011. Mapping human cortical areas *in vivo* based on myelin content as revealed by T1-and T2-weighted MRI. J. Neurosci. 31, 11597–11616. https://doi.org/10.1523/JNEUROSCI.2180-11.2011.

Glasser, M.F., Sotiropoulos, S.N., Wilson, J.A., Coalson, T.S., Fischl, B., Andersson, J.L., Xu, J., Jbabdi, S., Webster, M., Polimeni, J.R., 2013. The minimal preprocessing pipelines for the Human Connectome Project. Neuroimage 80, 105–124. https://doi.org/10.1016/j.neuroimage.2013.04.127.

Gouveia, F.V., Silk, E., Davidson, B., Pople, C.B., Abrahao, A., Hamilton, J., Ibrahim, G. M., Müller, D.J., Giacobbe, P., Lipsman, N., Hamani, C., 2021. A systematic review on neuromodulation therapies for reducing body weight in patients with obesity. Obes. Rev. 22 (10), e13309. https://doi.org/10.1111/obr.13309.

Greicius, M.D., Krasnow, B., Reiss, A.L., Menon, V., 2003. Functional connectivity in the resting brain: a network analysis of the default mode hypothesis. Proc. Natl. Acad. Sci. U. S. A. 100, 253–258. https://doi.org/10.1073/pnas.0135058100.

Gunderson, E.P., 2009. Childbearing and obesity in women: weight before, during, and after pregnancy. Obstet. Gynecol. Clin. 36, 317–332. https://doi.org/10.1016/j.ogc.2009.04.001.

Hamer, M., Batty, G.D., 2019. Association of body mass index and waist-to-hip ratio with brain structure: UK Biobank study. Neurology 92, e594–e600. https://doi.org/10.1212/WNL.0000000000006879.

Han, S., Cui, Q., Zheng, R., Li, S., Zhou, B., Fang, K., Sheng, W., Wen, B., Liu, L., Wei, Y., 2023a. Parsing altered gray matter morphology of depression using a framework integrating the normative model and non-negative matrix factorization. Nat. Commun. 14, 4053. https://doi.org/10.1038/s41467-023-39861-z.

Han, S., Xue, K., Chen, Y., Xu, Y., Li, S., Song, X., Guo, H.R., Fang, K., Zheng, R., Zhou, B., 2023b. Identification of shared and distinct patterns of brain network abnormality across mental disorders through individualized structural covariance network analysis. Psychol. Med. 1–12. https://doi.org/10.1017/S0033291723000302.

He, N., Rolls, E.T., Zhao, W., Guo, S., 2020. Predicting human inhibitory control from brain structural MRI. Brain Imaging Behav. 14, 2148–2158. https://doi.org/10.1007/s11682-019-00166-9.

Herrmann, M.J., Tesar, A.K., Beier, J., Berg, M., Warrings, B., 2019. Grey matter alterations in obesity: a meta-analysis of whole-brain studies. Obes. Rev. 20, 464–471. https://doi.org/10.1111/obr.12799.

Ho, D.E., Imai, K., King, G., Stuart, E.A., 2011. MatchIt: nonparametric preprocessing for parametric causal inference. J. Stat. Softw. 42, 1–28. https://doi.org/10.18637/jss.v042.i08.

Hofmann, W., Schmeichel, B.J., Baddeley, A.D., 2012. Executive functions and self-regulation. Trends Cogn. Sci. 16, 174–180. https://doi.org/10.1016/j.tics.2012.01.006.

Kim, A.Y., Shim, J.H., Choi, H.J., Baek, H.M., 2020. Comparison of volumetric and shape changes of subcortical structures based on 3-dimensional image between obesity and normal-weighted subjects using 3.0 T MRI. J. Clin. Neurosci. 73, 280–287. https://doi.org/10.1016/j.jocn.2019.12.052.

King, D.J., Wood, A.G., 2020. Clinically feasible brain morphometric similarity network construction approaches with restricted magnetic resonance imaging acquisitions. Netw. Neurosci. 4, 274–291. https://doi.org/10.1162/netn_a_00123.

Kivimäki, M., Strandberg, T., Pentti, J., Nyberg, S.T., Frank, P., Jokela, M., Ervasti, J., Suominen, S.B., Vahtera, J., Sipilä, P.N., 2022. Body-mass index and risk of obesity-related complex multimorbidity: an observational multicohort study. Lancet Diabetes Endocrinol. 10, 253–263. https://doi.org/10.1016/S2213-8587(22)00033-X.

Knudsen, E.B., Wallis, J.D., 2022. Taking stock of value in the orbitofrontal cortex. Nat. Rev. Neurosci. 23, 428–438. https://doi.org/10.1038/s41583-022-00589-2.

Kringelbach, M.L., Rolls, E.T., 2004. The functional neuroanatomy of the human orbitofrontal cortex: evidence from neuroimaging and neuropsychology. Prog. Neurobiol. 72, 341–372. https://doi.org/10.1016/j.pneurobio.2004.03.006.

Larivière, S., Paquola, C., Park, B.-y., Royer, J., Wang, Y., Benkarim, O., Vos de Wael, R., Valk, S.L., Thomopoulos, S.I., Kirschner, M., 2021. The ENIGMA Toolbox: multiscale neural contextualization of multisite neuroimaging datasets. Nat. Methods 18, 698–700. https://doi.org/10.1038/s41592-021-01186-4.

Laurent, J.S., Watts, R., Adise, S., Allgaier, N., Chaarani, B., Garavan, H., Potter, A., Mackey, S., 2020. Associations among body mass index, cortical thickness, and executive function in children. JAMA Pediatr. 174, 170–177. https://doi.org/10.1001/jamapediatrics.2019.4708.

Li, W., Yang, C., Shi, F., Wu, S., Wang, Q., Nie, Y., Zhang, X., 2017. Construction of individual morphological brain networks with multiple morphometric features. Front. Neuroanat. 11 (34) https://doi.org/10.3389/fnana.2017.00034.

Li, J., Seidlitz, J., Suckling, J., Fan, F., Ji, G.J., Meng, Y., Yang, S., Wang, K., Qiu, J., Chen, H., 2021. Cortical structural differences in major depressive disorder correlate with cell type-specific transcriptional signatures. Nat. Commun. 12, 1647. https://doi.org/10.1038/s41467-021-21943-5.

Li, W., Chen, X., Luo, Y., Luo, L., Chen, H., 2022. Orbitofrontal neural dissociation of healthy and unhealthy food reward sensitivity in normal-weight binge eaters. Psychiatry Res. 316, 114736 https://doi.org/10.1016/j.psychres.2022.114736.

Li, G., Hu, Y., Zhang, W., Wang, J., Ji, W., Manza, P., Volkow, N.D., Zhang, Y., Wang, G. J., 2023. Brain functional and structural magnetic resonance imaging of obesity and weight loss interventions. Mol. Psychiatry 28, 1466–1479. https://doi.org/10.1038/s41380-023-02025-y.

Lips, M.A., Wijngaarden, M.A., van der Grond, J., van Buchem, M.A., de Groot, G.H., Rombouts, S.A., Pijl, H., Veer, I.M., 2014. Resting-state functional connectivity of brain regions involved in cognitive control, motivation, and reward is enhanced in obese females. Am. J. Clin. Nutr. 100, 524–531. https://doi.org/10.3945/ajcn.113.080671.

Lowe, C.J., Reichelt, A.C., Hall, P.A., 2019. The prefrontal cortex and obesity: a health neuroscience perspective. Trends Cogn. Sci. 23, 349–361. https://doi.org/10.1016/j.tics.2019.01.005.

Lowe, C.J., Morton, J.B., Reichelt, A.C., 2020. Adolescent obesity and dietary decision making—A brain-health perspective. Lancet Child Adolesc. Health 4, 388–396. https://doi.org/10.1016/S2352-4642(19)30404-3.

Mar, A.C., Walker, A.L., Theobald, D.E., Eagle, D.M., Robbins, T.W., 2011. Dissociable effects of lesions to orbitofrontal cortex subregions on impulsive choice in the rat. J. Neurosci. 31, 6398–6404. https://doi.org/10.1523/JNEUROSCI.6620-10.2011.

Marqués-Iturria, I., Pueyo, R., Garolera, M., Segura, B., Junqué, C., García-García, I., Sender-Palacios, M.J., Vernet-Vernet, M., Narberhaus, A., Ariza, M., 2013. Frontal cortical thinning and subcortical volume reductions in early adulthood obesity. Psychiatry Res. Neuroimaging 214, 109–115. https://doi.org/10.1016/j.pscychresns.2013.06.004.

May, M., Schindler, C., Engeli, S., 2020. Modern pharmacological treatment of obese patients. Ther. Adv. Endocrinol. Metab. 11 https://doi.org/10.1177/2042018819897527, 2042018819897527.

McClure, S.M., Ericson, K.M., Laibson, D.I., Loewenstein, G., Cohen, J.D., 2007. Time discounting for primary rewards. J. Neurosci. 27, 5796–5804. https://doi.org/10.1523/JNEUROSCI.4246-06.2007.

Michel, L.C., McCormick, E.M., Kievit, R.A., 2024. Grey and white matter metrics demonstrate distinct and complementary prediction of differences in cognitive performance in children: findings from ABCD (N= 11 876). J. Neurosci., e0465232023 https://doi.org/10.1523/JNEUROSCI.0465-23.2023.

Morgan, S.E., Seidlitz, J., Whitaker, K.J., Romero-Garcia, R., Clifton, N.E., Scarpazza, C., Van Amelsvoort, T., Marcelis, M., Van Os, J., Donohoe, G., 2019. Cortical patterning

of abnormal morphometric similarity in psychosis is associated with brain expression of schizophrenia-related genes. Proc. Natl. Acad. Sci. U. S. A. 116, 9604–9609. https://doi.org/10.1073/pnas.1820754116.
Noonan, M., Walton, M., Behrens, T., Sallet, J., Buckley, M., Rushworth, M., 2010. Separate value comparison and learning mechanisms in macaque medial and lateral orbitofrontal cortex. Proc. Natl. Acad. Sci. U. S. A. 107, 20547–20552. https://doi.org/10.1073/pnas.1012246107.
Nota, M.H., Vreeken, D., Wiesmann, M., Aarts, E.O., Hazebroek, E.J., Kiliaan, A.J., 2020. Obesity affects brain structure and function-rescue by bariatric surgery? Neurosci. Biobehav. Rev. 108, 646–657. https://doi.org/10.1016/j.neubiorev.2019.11.025.
Okudzhava, L., Heldmann, M., Münte, T.F., 2022. A systematic review of diffusion tensor imaging studies in obesity. Obes. Rev. 23, e13388. https://doi.org/10.1111/obr.13388.
Opel, N., Redlich, R., Kaehler, C., Grotegerd, D., Dohm, K., Heindel, W., Kugel, H., Thalamuthu, A., Koutsouleris, N., Arolt, V., 2017. Prefrontal gray matter volume mediates genetic risks for obesity. Mol. Psychiatry 22, 703–710. https://doi.org/10.1038/mp.2017.51.
Parsons, N., Steward, T., Clohesy, R., Almgren, H., Duehlmeyer, L., 2022. A systematic review of resting-state functional connectivity in obesity: refining current neurobiological frameworks and methodological considerations moving forward. Rev. Endocr. Metab. Disord. 23, 861–879. https://doi.org/10.1007/s11154-021-09665-x.
Plotnikoff, R.C., Costigan, S.A., Williams, R.L., Hutchesson, M.J., Kennedy, S.G., Robards, S.L., Allen, J., Collins, C.E., Callister, R., Germov, J., 2015. Effectiveness of interventions targeting physical activity, nutrition and healthy weight for university and college students: a systematic review and meta-analysis. Int. J. Behav. Nutr. Phys. Act. 12, 1–10. https://doi.org/10.1186/s12966-015-0203-7.
Reinehr, T., 2010. Obesity and thyroid function. Mol. Cell. Endocrinol. 316, 165–171. https://doi.org/10.1016/j.mce.2009.06.005.
Rolls, E.T., Deco, G., Huang, C.C., Feng, J., 2023a. Human amygdala compared to orbitofrontal cortex connectivity, and emotion. Prog. Neurobiol. 220, 102385 https://doi.org/10.1016/j.pneurobio.2022.102385.
Rolls, E.T., Feng, R., Cheng, W., Feng, J., 2023b. Orbitofrontal cortex connectivity is associated with food reward and body weight in humans. Soc. Cogn. Affect. Neurosci. 18 https://doi.org/10.1093/scan/nsab083 nsab083.
Rolls, E.T., 2023. The orbitofrontal cortex, food reward, body weight and obesity. Soc. Cogn. Affect. Neurosci. 18 https://doi.org/10.1093/scan/nsab044 nsab044.
Romero-Garcia, R., Atienza, M., Clemmensen, L.H., Cantero, J.L., 2012. Effects of network resolution on topological properties of human neocortex. Neuroimage 59, 3522–3532. https://doi.org/10.1016/j.neuroimage.2011.10.086.
Ronan, L., Alexander-Bloch, A., Fletcher, P.C., 2020. Childhood obesity, cortical structure, and executive function in healthy children. Cereb. Cortex 30, 2519–2528. https://doi.org/10.1093/cercor/bhz257.
Sabuncu, M.R., Ge, T., Holmes, A.J., Smoller, J.W., Buckner, R.L., Fischl, B., Initiative, A. s.D.N., 2016. Morphometricity as a measure of the neuroanatomical signature of a trait. Proc. Natl. Acad. Sci. U. S. A. 113, E5749–E5756. https://doi.org/10.1073/pnas.1604378113.
Sadler, J.R., Shearrer, G.E., Burger, K.S., 2018. Body mass variability is represented by distinct functional connectivity patterns. Neuroimage 181, 55–63. https://doi.org/10.1016/j.neuroimage.2018.06.082.
Salehinejad, M.A., Ghanavati, E., Rashid, M.H.A., Nitsche, M.A., 2021. Hot and cold executive functions in the brain: a prefrontal-cingular network. Brain Neurosci. Adv. 5, 23982128211007769 https://doi.org/10.1177/23982128211007769.
Schlögl, H., Horstmann, A., Villringer, A., Stumvoll, M., 2016. Functional neuroimaging in obesity and the potential for development of novel treatments. Lancet Diabetes Endocrinol. 4, 695–705. https://doi.org/10.1016/S2213-8587(15)00475-1.
Seabrook, L.T., Borgland, S.L., 2020. The orbitofrontal cortex, food intake and obesity. J. Psychiatry Neurosci. 45, 304–312. https://doi.org/10.1503/jpn.190163.
Seidlitz, J., Váša, F., Shinn, M., Romero-Garcia, R., Whitaker, K.J., Vértes, P.E., Wagstyl, K., Reardon, P.K., Clasen, L., Liu, S., 2018. Morphometric similarity networks detect microscale cortical organization and predict inter-individual cognitive variation. Neuron 97, 231–247. https://doi.org/10.1016/j.neuron.2017.11.039 e237.
Smith, K.E., Luo, S., Mason, T.B., 2021. A systematic review of neural correlates of dysregulated eating associated with obesity risk in youth. Neurosci. Biobehav. Rev. 124, 245–266. https://doi.org/10.1016/j.neubiorev.2021.02.013.
Smucny, J., Cornier, M.A., Eichman, L.C., Thomas, E.A., Bechtell, J.L., Tregellas, J.R., 2012. Brain structure predicts risk for obesity. Appetite 59, 859–865. https://doi.org/10.1016/j.appet.2012.08.027.
Snoek, L., van der Miesen, M.M., Beemsterboer, T., Van Der Leij, A., Eigenhuis, A., Steven Scholte, H., 2021. The Amsterdam Open MRI Collection, a set of multimodal MRI datasets for individual difference analyses. Sci. Data 8 (85). https://doi.org/10.1038/s41597-021-00870-6.
Stice, E., Burger, K., 2019. Neural vulnerability factors for obesity. Clin. Psychol. Rev. 68, 38–53. https://doi.org/10.1016/j.cpr.2018.12.002.
Stice, E., Yokum, S., 2016. Neural vulnerability factors that increase risk for future weight gain. Psychol. Bull. 142 (447) https://doi.org/10.1037/bul0000044.
Stice, E., Shaw, H., Marti, C.N., 2006. A meta-analytic review of obesity prevention programs for children and adolescents: the skinny on interventions that work. Psychol. Bull. 132 (667) https://doi.org/10.1037/0033-2909.132.5.667.
Stuart, E.A., Green, K.M., 2008. Using full matching to estimate causal effects in nonexperimental studies: examining the relationship between adolescent marijuana use and adult outcomes. Dev. Psychol. 44 (395) https://doi.org/10.1037/0012-1649.44.2.395.
Syan, S.K., McIntyre-Wood, C., Minuzzi, L., Hall, G., McCabe, R.E., MacKillop, J., 2021. Dysregulated resting state functional connectivity and obesity: a systematic review. Neurosci. Biobehav. Rev. 131, 270–292. https://doi.org/10.1016/j.neubiorev.2021.08.019.
Uddin, L.Q., 2013. Complex relationships between structural and functional brain connectivity. Trends Cogn. Sci. 17, 600–602. https://doi.org/10.1016/j.tics.2013.09.011.
Váša, F., Seidlitz, J., Romero-Garcia, R., Whitaker, K.J., Rosenthal, G., Vértes, P.E., Shinn, M., Alexander-Bloch, A., Fonagy, P., Dolan, R.J., 2018. Adolescent tuning of association cortex in human structural brain networks. Cereb. Cortex 28, 281–294. https://doi.org/10.1093/cercor/bhx249.
Valk, S.L., Xu, T., Margulies, D.S., Masouleh, S.K., Paquola, C., Goulas, A., Kochunov, P., Smallwood, J., Yeo, B.T., Bernhardt, B.C., 2020. Shaping brain structure: genetic and phylogenetic axes of macroscale organization of cortical thickness. Sci. Adv. 6, eabb3417. https://doi.org/10.1126/sciadv.abb3417.
Van Essen, D.C., Smith, S.M., Barch, D.M., Behrens, T.E., Yacoub, E., Ugurbil, K., WU-Minn HCP Consortium, 2013. The WU-Minn human connectome project: an overview. Neuroimage 80, 62–79. https://doi.org/10.1016/j.neuroimage.2013.05.041.
Vandekar, S.N., Shinohara, R.T., Raznahan, A., Hopson, R.D., Roalf, D.R., Ruparel, K., Gur, R.C., Gur, R.E., Satterthwaite, T.D., 2016. Subject-level measurement of local cortical coupling. Neuroimage 133, 88–97. https://doi.org/10.1016/j.neuroimage.2016.03.002.
Wang, M.Z., Hayden, B.Y., Heilbronner, S.R., 2022. A structural and functional subdivision in central orbitofrontal cortex. Nat. Commun. 13, 3623. https://doi.org/10.1038/s41467-022-31273-9.
Wang, Y., Dong, D., Chen, X., Gao, X., Liu, Y., Xiao, M., Guo, C., Chen, H., 2023. Individualized morphometric similarity predicts body mass index and food approach behavior in school-age children. Cereb. Cortex 33, 4794–4805. https://doi.org/10.1093/cercor/bhac380.
Weafer, J., Crane, N.A., Gorka, S.M., Phan, K.L., de Wit, H., 2019. Neural correlates of inhibition and reward are negatively associated. Neuroimage 196, 188–194. https://doi.org/10.1016/j.neuroimage.2019.04.021.
Wei, Y., Scholtens, L.H., Turk, E., Van Den Heuvel, M.P., 2018. Multiscale examination of cytoarchitectonic similarity and human brain connectivity. Netw. Neurosci. 3, 124–137. https://doi.org/10.1162/netn_a_00057.
Whitaker, K.J., Vértes, P.E., Romero-Garcia, R., Váša, F., Moutoussis, M., Prabhu, G., Weiskopf, N., Callaghan, M.F., Wagstyl, K., Rittman, T., 2016. Adolescence is associated with genomically patterned consolidation of the hubs of the human brain connectome. Proc. Natl. Acad. Sci. U. S. A. 113, 9105–9110. https://doi.org/10.1073/pnas.1601745113.
Winkler, A.M., Ridgway, G.R., Webster, M.A., Smith, S.M., Nichols, T.E., 2014. Permutation inference for the general linear model. Neuroimage 92, 381–397. https://doi.org/10.1016/j.neuroimage.2014.01.060.
World Health Organization, 2024. Obesity and overweight. https://www.who.int/news-room/fact-sheets/detail/obesity-and-overweight (accessed March 1, 2024).
Xia, M., Wang, J., He, Y., 2013. BrainNet Viewer: a network visualization tool for human brain connectomics. PLoS One 8, e68910. https://doi.org/10.1371/journal.pone.0068910.
Yan, W., Bingxian, H., Hua, Y., Jianghong, D., Jun, C., Dongliang, G., Yujian, Z., Ling, L., Yanying, G., Kaiti, X., 2007. Waist-to-height ratio is an accurate and easier index for evaluating obesity in children and adolescents. Obesity 15, 748–752. https://doi.org/10.1038/oby.2007.601.
Yang, Y., Shields, G.S., Guo, C., Liu, Y., 2018. Executive function performance in obesity and overweight individuals: a meta-analysis and review. Neurosci. Biobehav. Rev. 84, 225–244. https://doi.org/10.1016/j.neubiorev.2017.11.020.
Yang, S., Wagstyl, K., Meng, Y., Zhao, X., Li, J., Zhong, P., Li, B., Fan, Y.S., Chen, H., Liao, W., 2021. Cortical patterning of morphometric similarity gradient reveals diverged hierarchical organization in sensory-motor cortices. Cell Rep. 36 https://doi.org/10.1016/j.celrep.2021.109582.
Yeo, B.T., Krienen, F.M., Sepulcre, J., Sabuncu, M.R., Lashkari, D., Hollinshead, M., Roffman, J.L., Smoller, J.W., Zöllei, L., Polimeni, J.R., 2011. The organization of the human cerebral cortex estimated by intrinsic functional connectivity. J. Neurophysiol. 106, 1125–1165. https://doi.org/10.1152/jn.00338.2011.
Yu, K., Wang, X., Li, Q., Zhang, X., Li, X., Li, S., 2018. Individual morphological brain network construction based on multivariate euclidean distances between brain regions. Front. Hum. Neurosci. 12 (204) https://doi.org/10.3389/fnhum.2018.00204.
Zapparoli, L., Devoto, F., Giannini, G., Zonca, S., Gallo, F., Paulesu, E., 2022. Neural structural abnormalities behind altered brain activation in obesity: evidence from meta-analyses of brain activation and morphometric data. NeuroImage Clin 36, 103179. https://doi.org/10.1016/j.nicl.2022.103179.
Zeng, B.Y., Zeng, B.S., Chen, Y.W., Hung, C.M., Sun, C.K., Cheng, Y.S., Stubbs, B., Carvalho, A.F., Brunoni, A.R., Su, K.P., 2021. Efficacy and acceptability of noninvasive brain stimulation interventions for weight reduction in obesity: a pilot network meta-analysis. Int. J. Obes. 45, 1705–1716. https://doi.org/10.1038/s41366-021-00833-2.
Zhang, W., Ji, G., Manza, P., Li, G., Hu, Y., Wang, J., Lv, G., He, Y., von Deneen, K.M., Han, Y., 2021a. Connectome-based prediction of optimal weight loss six months after bariatric surgery. Cereb. Cortex 31, 2561–2573. https://doi.org/10.1093/cercor/bhaa374.
Zhang, Y., Ma, M., Xie, Z., Wu, H., Zhang, N., Shen, J., 2021b. Bridging the gap between morphometric similarity mapping and gene transcription in alzheimer's disease. Front. Neurosci. 15, 731292 https://doi.org/10.3389/fnins.2021.731292.
Zhang, Z., Robinson, L., Jia, T., Quinlan, E.B., Tay, N., Chu, C., Barker, E.D., Banaschewski, T., Barker, G.J., Bokde, A.L., 2021c. Development of disordered eating behaviors and comorbid depressive symptoms in adolescence: neural and

psychopathological predictors. Biol. Psychiatry 90, 853–862. https://doi.org/10.1016/j.biopsych.2020.06.003.